

Application of the Linear Spectral Mixture Model in vegetation change detection based on the Green Vegetation Index

Alindomar Lacerda Silva¹
Catherine Torres de Almeida¹
Natália Cristina Wiederkehr¹
Renata Maciel Ribeiro¹
Thales Sehn Körting¹

Instituto Nacional de Pesquisas Espaciais¹
Caixa Postal 515 - 12227-010 - São José dos Campos - SP, Brasil
{alindomar.silva, catherine.almeida, natalia.wiederkehr, renata.ribeiro, thales.korting}@inpe.br;

Abstract. The Amazon forest, which is one of the main tropical forests in the globe, has been undergoing to anthropogenic pressure, what could lead to forest loss and degradation. As a consequence, public policies focusing on preservation, conservation and monitoring are mandatory, especially in protected areas. The use of satellite imagery allows a better understanding of how human activities are causing land use and land cover change (LULCC). The aim of this study is to identify land cover change from 2001 to 2004, inside and outside the National Forest of Tapajós (FLONA Tapajós), using the Linear Spectral Mixture Model (LSMM) and a Green Vegetation (GV) index. Results showed that the biggest changes between 2001 and 2004 occurred outside the FLONA. The GV Index was more suited to detect small losses of vegetation than the GV fraction alone.

Key-words: remote sensing, image processing, land use and land cover change.

1. Introduction

In the Amazon Forest the processes involving land use and land cover change (LULCC) are restricted primarily to the last 30 years, with most deforestation concentrated along the southern and eastern flanks of the region, in an area termed as “arc of deforestation” or “arc of fire”, which is an area where timber extraction, deforestation, fires and agriculture expansion occurs (Becker, 2009). These processes are associated with many factors, both anthropogenic (e. g. urbanization, agricultural expansion, etc.) and natural (such as droughts, extreme weather), and lead to change and complete conversion of the forest onto other land cover types (IBAMA, 2004). Due to the fact that changes in the Amazon could affect biodiversity, carbon cycle, hydrological balance, climate control and other services, it is important to maintain an assiduous monitoring in Amazonian vegetated areas.

Usually these changes are difficult to measure; therefore remote sensing has played an important role in mapping land cover and quantifying change in the Amazon for more than 25 years (Potter et al., 1993; Running et al., 1999). The techniques used in remote sensing image processing are of great importance to identify, detect and extract information. Furthermore, these techniques would be helpful for surveillance promoted by environmental agencies, especially in sizeable areas as the Amazon Forest. Many LULCC detection techniques were developed using remote sensing images (Kennedy et al., 2009), however, most of these researches focus on conversion processes, such as changes from forest to agriculture, in relation to modification processes, such as degradation and growth (Lu et al., 2014).

The purpose of this study is the evaluation of vegetation changes from 2001 to 2004 inside and outside the Tapajós National Forest. For this, we used the Linear Spectral Mixture Model (LSMM), based on the methodology developed by Lu et al. (2014).

2. Methodology

2.1. Study Area

This study was conducted in the northern area of the Tapajós National Forest (FLONA), Figure 1, south of Santarém municipality, Pará state, Brazil, next to BR 163 highway, which connects Cuiabá (Mato Grosso state) to Santarém.

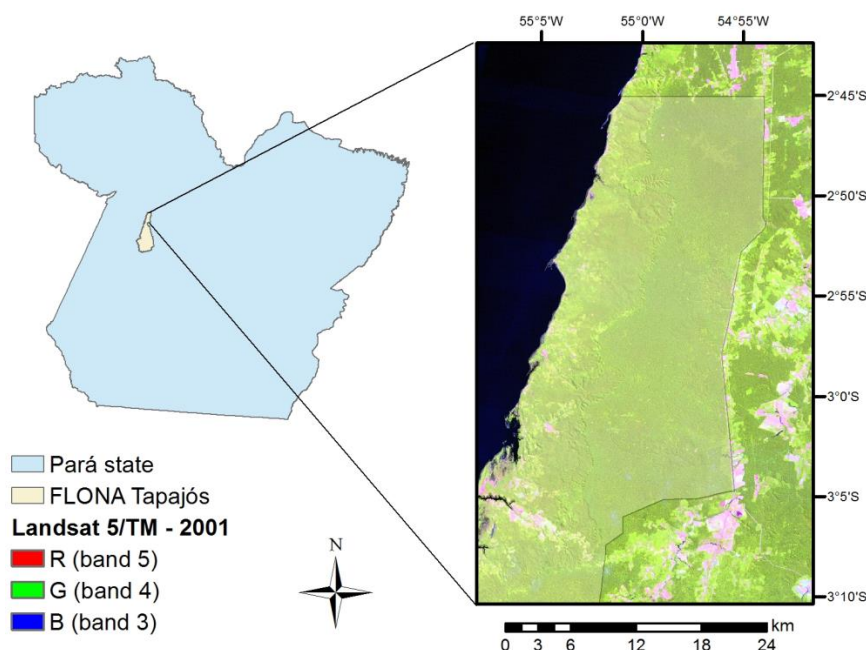


Figure 1. FLONA Tapajós location.

The area is mainly covered by primary forest, but some areas within the FLONA, located in the south of the studied area, are ceded to selective logging. For example, in September 2001 underwent through a selective logging. The logging was managed by the Brazilian Institute for the Environment and Renewable Resources (IBAMA) and participated of a reduced-impact-logging project over a 5-year period beginning in 1999 (Figueira et al., 2008). This logging episode may cause slight changes inside the FLONA. The area chosen for this study also contains an area outside the FLONA borders, to the east of the BR 163 highway, characterized by the presence of secondary forests, cattle raising and agriculture. These activities might cause greater variations in LULCC.

The average annual precipitation was approximately 1900 mm, with a distinct wet season between January and June, and a dry season between July and December. The maximum daily temperature was 24° to 32°C and the minimum was 20° to 25°C (Figueira et al., 2008).

2.2. Input data

In order to detect changes in vegetation, we used two images from Landsat-5 TM sensor (with a spatial resolution of 30 meters), acquired in August 07, 2001, previous a logging episode, and July 30, 2004, after the logging. Minimal cloud cover and great visual range were the criteria used to choose the images.

The images were retrieved from the *U.S. Geological Survey - Earth Explorer* catalog (<http://earthexplorer.usgs.gov/>), already converted to surface reflectance values. They were also downloaded already with geometric and radiometric corrections. In addition to the six Landsat-5 TM bands surface reflectance, a “cfmask” was used to identify areas with cloud, cloud shadow, snow and water. This mask was applied to detect cloud covered and shadowed areas, excluding them from the final result due to the lack they would cause in vegetation cover data.

The path and row of the study area were 227 and 062, respectively. Further, the images were clipped in order to contain only the area of interest. The FLONA boundaries were acquired at ICMBIO online database (<http://www.icmbio.gov.br/portal/geoprocessamentos>).

To extract the FLONA polygon (contour), the software quantum GIS was used, but for the other steps in image processing ENVI 5.1 was employed. The main methodological procedures used in this study are summarized in Figure 2.

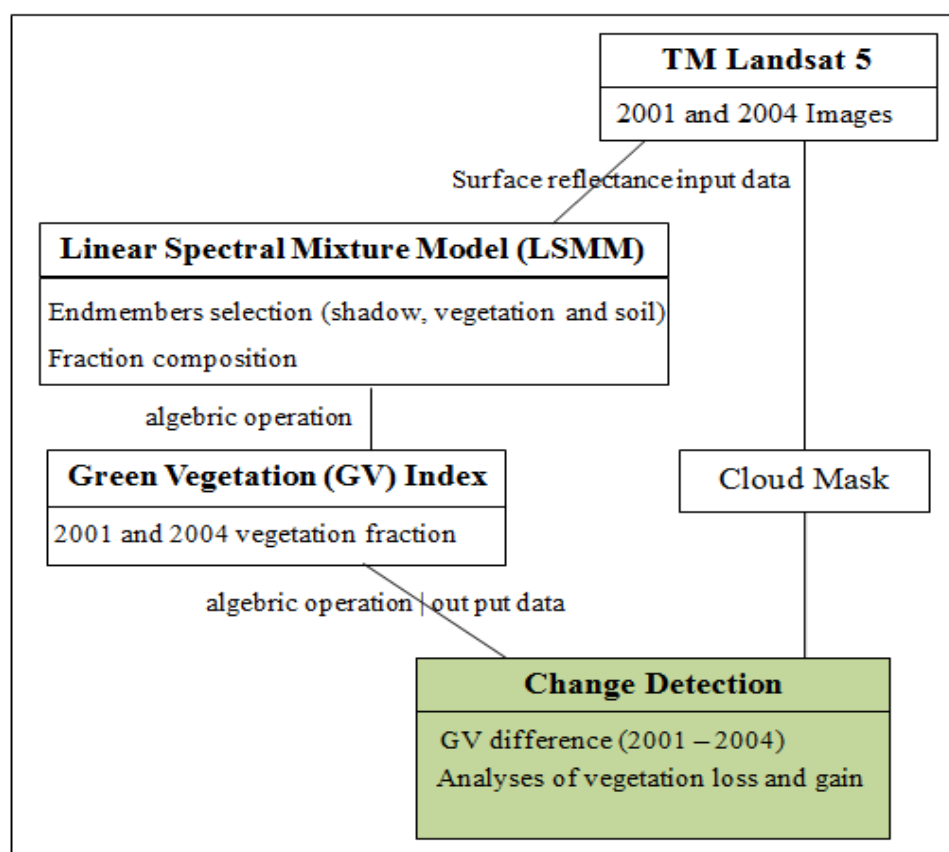


Figure 2. Main diagram of the employed methodology.

2.3. Linear Spectral Mixture Model (LSMM)

The LSMM considers that the reflectance in each pixel is a linear combination spectra of all the components within the pixel (Shimabukuro e Smith, 1991; Adams et al., 1995), weighted by the fraction of each component, as in equation 1.

$$R_i = \sum_{j=1}^n (f_j R_{ij}) + e_i \quad (1)$$

Where R_i is the pixel reflectance in band i ; R_{ij} is the reflectance of an endmember j in band i ; f_j is the fraction occupied by endmember j within the pixel and e_i is the error of band i . It is assumed that the sum of the fractions must equal 1.

This model creates synthetic images that represent each component's proportion within an image pixel. The number of bands is reduced to the number of components used in the model, which reduces the volume of data. For this study, three endmembers were chosen, green vegetation (GV), soil and shadow, as expressed in equation 2:

$$R_i = f_{GV} * R_{GV_i} + f_{soil} * R_{soil_i} + f_{shadow} * R_{shadow_i} + e_i \quad (2)$$

To find the endmembers, a 2D scatterplot of the red (x axis) and near infrared (y axis) bands was created. The analysis of the scatterplot allowed the identification of clusters that represent each component's spectral behavior (soil, vegetation and shadow). After selection, a false composite RGB (5,4,3) was made, enabling the choice of samples for each component to generate the image fractions from the LSMM.

The steps described above were applied in both images; since, according to Smith et. al. (1990), the values of pure components from the interest image are valid only for the scene they were picked from; therefore, they cannot be applied on other images, neither if the area is the same (but acquired with another sensor), nor under distinct illumination and atmospheric conditions.

With the results from the LSMM, the contribution of each component for the scene was then calculated. For this study's purposes, only the vegetation fraction was taken into account for detecting vegetation changes.

2.4. Green Vegetation Index and Change Detection

According to Lu et al. (2014), the GV index (equation 3) is used to detect vegetation gain and loss, as well as identify small variations in the vegetation.

$$GVindex = \frac{f_{GV}}{1.1 - f_{GV}} \quad (3)$$

This index varies between 0 and 10. The value 1.1 in equation 3 is to avoid 0 values in the denominator, just in case the vegetation fraction equals to 1. Having an exponential relationship with the vegetation fraction (f_{GV}) small changes are enlarged by using GV index (Lu et al., 2014).

For the purpose of finding vegetation loss and gain, the difference between 2001 and 2004 GV index was calculated. As a result, values near zero indicate no change, positive values points to vegetation loss and negative values show a gain in vegetation. Still, it was a need to establish thresholds which would allow to identify areas with no change, large changes and small changes (gain and loss) caused by conversion and modification. For selecting the thresholds, the histogram of the difference image was divided in five regions, two of loss (small and large), two of gain and one of no change, based in its statistical parameters mode and standard deviation. The distances of 1.5 and 3 standard deviations in relation to the mode were used as thresholds (Figure 3b).

The mode was chosen rather than the average, because as the change detection was established for images with short time interval, the average is shifted to the vegetation loss region, generating an asymmetric histogram. In contrast, the mode, which corresponds to the zero value, is centered in the no change class.

In order to compare the results obtained with the GV Index, a map with the vegetation fraction (f_{GV}) difference was made, using the same procedures to choose the thresholds (Figure 3a).

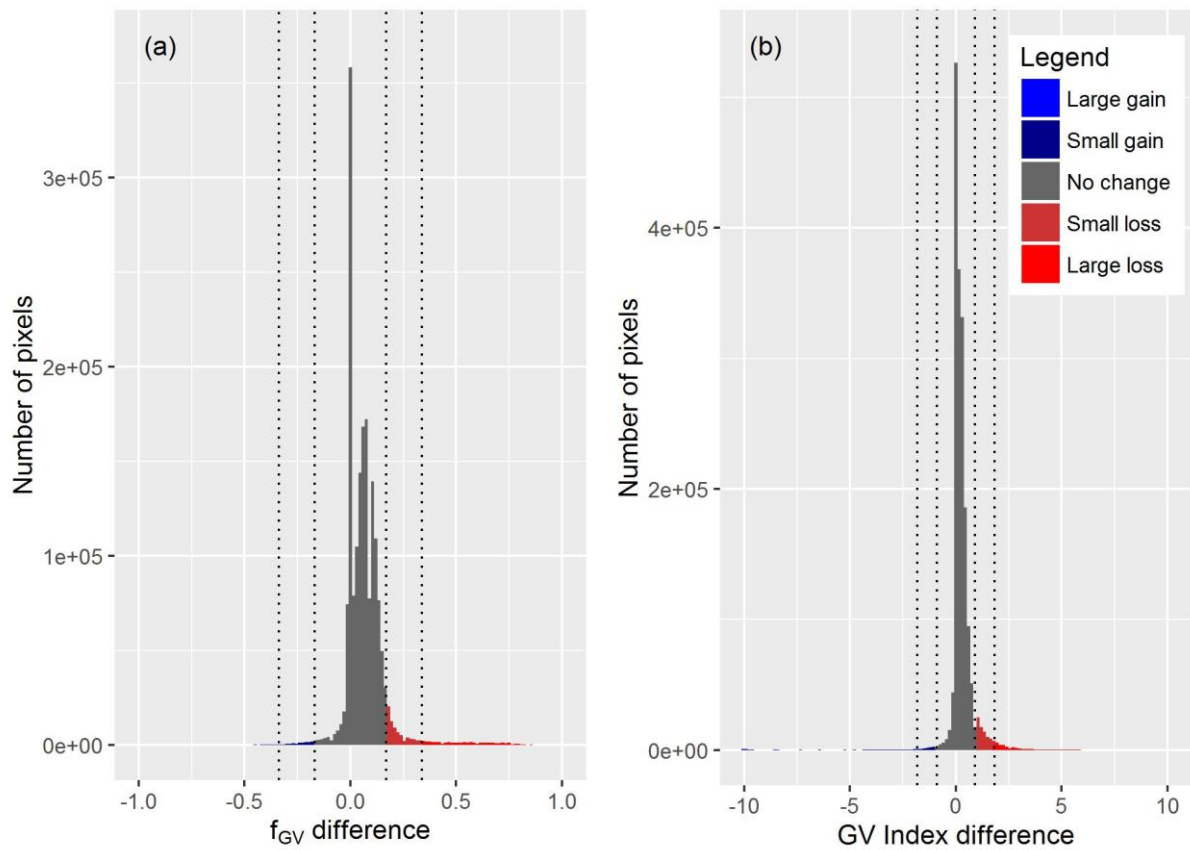


Figure 3. Histogram of vegetation fraction (f_{GV}) difference (a) and GV Index difference (b). The dotted lines represent the thresholds.

3. Results and Discussion

Figure 4 shows a colored composite of the three fractions derived from the LSM for 2001 and 2004. It is possible to distinguish exposed soil (in red), water bodies (in blue) and predominantly green vegetation (in green). The cloudy areas in the image of 2004 were excluded from the analysis of land cover change detection, in order to improve final results.

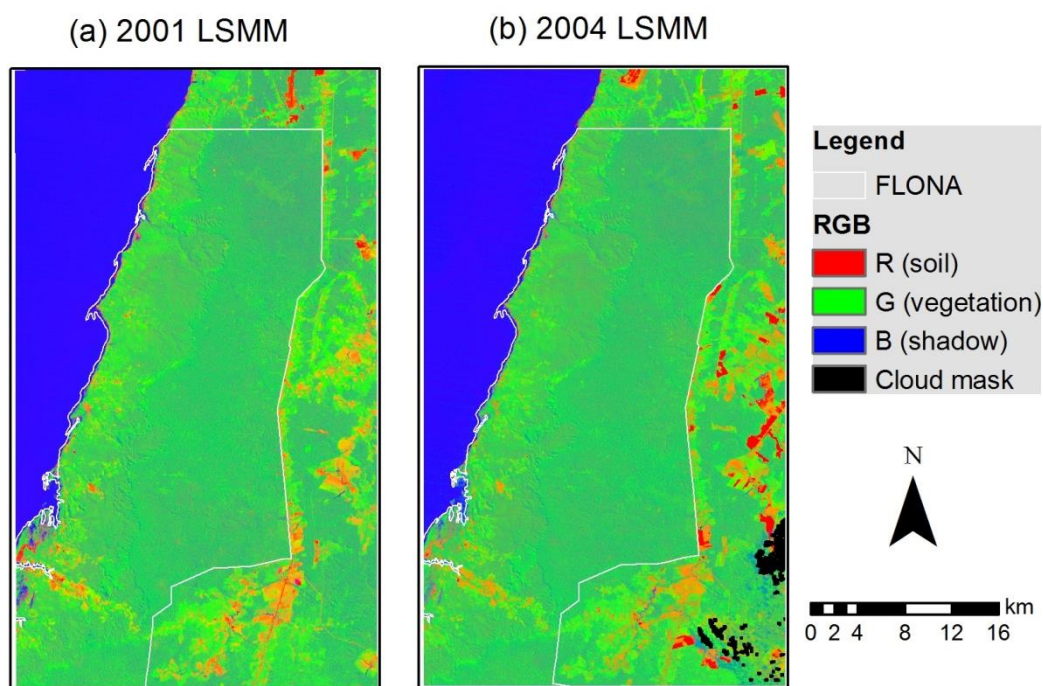


Figure 4. Colored composite of the three fractions (soil, vegetation and shadow) derived from the LSMM for 2001 (a) and 2004 (b).

The 2001 and 2004 vegetation fractions derived from the Linear Spectral Mixture Model are presented in Figure 5 a and b. Clear pixels represent areas composed mainly by vegetation (values near 1). These areas are usually associated with undergrowth vegetation (shrubs and saplings). Forested areas were the ones with intermediate values due to major contribution of the shadow fraction. Dark pixels are associated with bare soil, clouds or water, without vegetation. The GV index images (Figure 5 c and d) exhibited similar patterns, with the clearest pixels representing vegetation and the darkest pixels soil and shadow. Nonetheless, the GV Index varies between 0 and 10. When comparing the vegetation fraction and the GV index from both years, it is possible to notice land cover changes, especially in the eastern region, outside the FLONA borders.

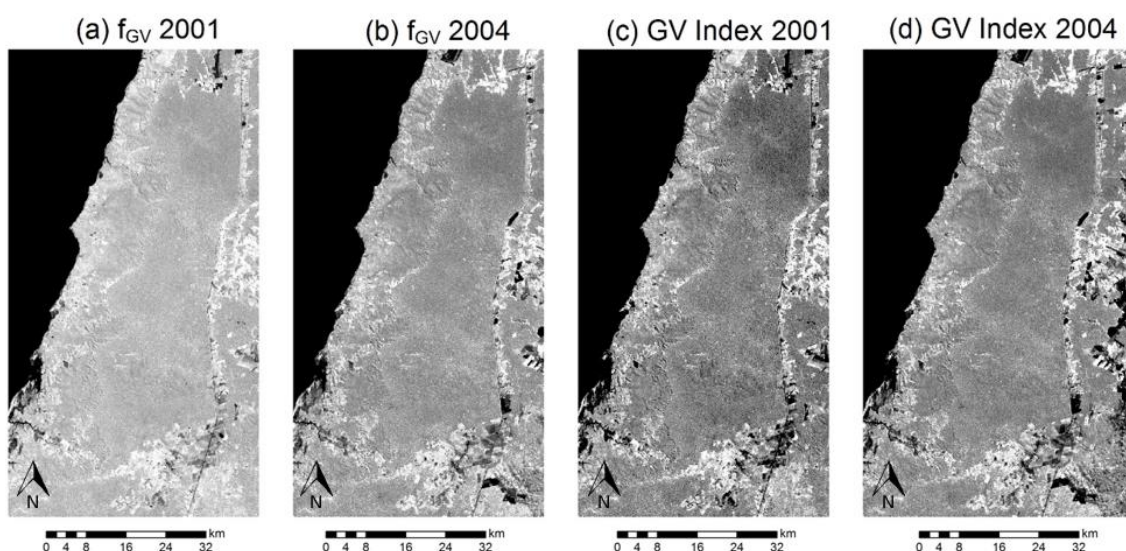


Figure 5. Vegetation fraction and GV Index of the years 2001 and 2004.

Maps with the vegetation fraction (f_{GV}) and GV index difference between 2001 and 2004 are showed in Figure 6. These maps highlight changes in vegetation, gain in blue and loss in red color. Most part of the area; however, has not changed. The area within the FLONA limits displayed small changes, which is probably related to vegetation loss caused by a logging episode in September 2001. Changes outside the FLONA limits are mostly associated with phenological stages of plantations, so these changes are not necessarily related to land cover change.

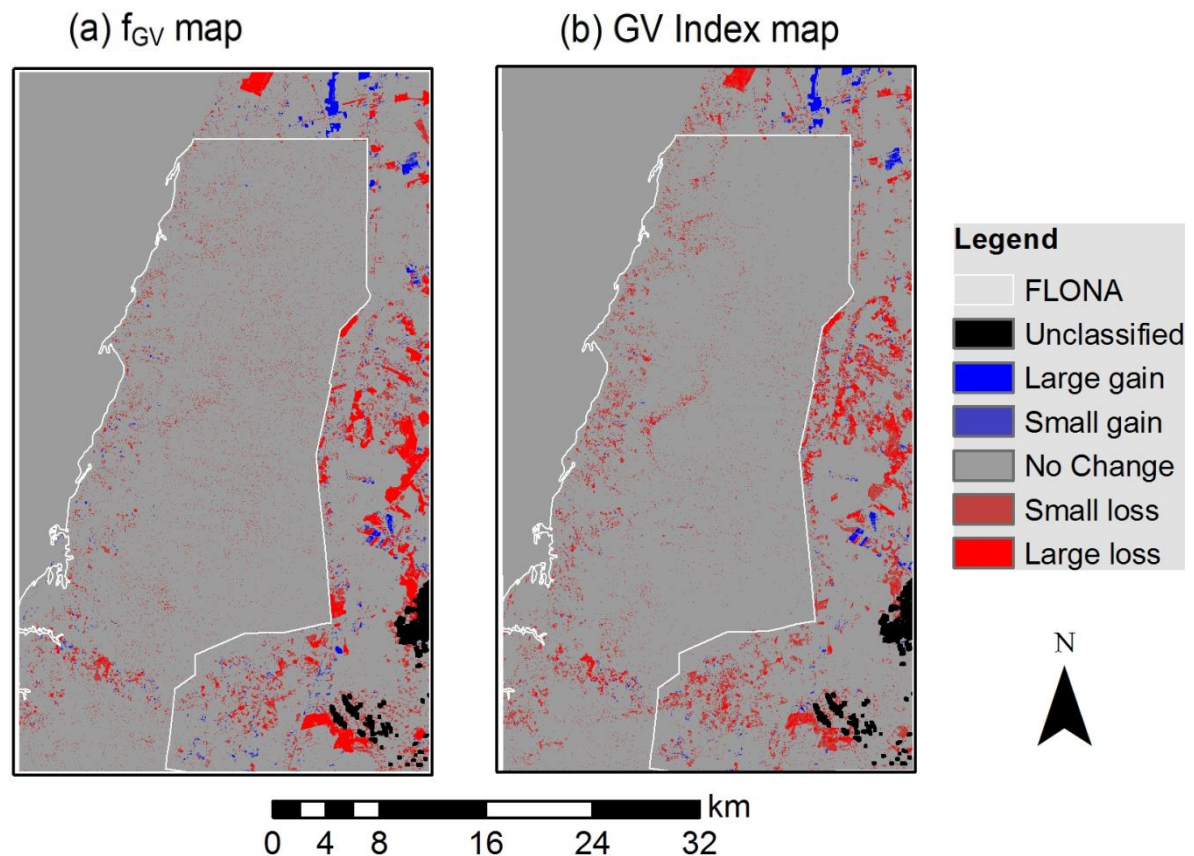


Figure 6. Vegetation fraction and GV index difference map.

Table 1 shows that by opposing the scope of the classification of the two methods, the GV Index showed higher sensitivity in the classification of small losses, increasing 7.88 km² of this class in relation to f_{GV} . Thus, the GV Index was more suited to detect small losses of vegetation. The f_{GV} was more sensitive to detect large changes, mainly to large losses. Moreover, the changes detected by f_{GV} within the area of the FLONA seems to apparently spread more throughout the area, while the GV Index appears detect more localized changes.

Table 1. Area of the classes derived by the f_{GV} and the GV Index

Classes	f_{GV}	GV Index	Difference
	Total Area (km ²)	Total Area (km ²)	Area (km ²)
Large gain	6.14	5.28	-0.86
Small gain	10.23	7.56	-2.66
No Change	1476.70	1485.65	8.95
Small loss	79.38	87.26	7.88
Large loss	41.93	28.62	-13.31

4. Final Remarks

By using the GV index it was possible to detect slight land cover changes in the study area, especially in vegetation, confirming its importance and relevance already observed by Lu et al. (2014). The association of the LSMM and the GV index was an important step on the detection of vegetation cover and condition changes.

The technique used in this study was useful to identify small changes within and outside the FLONA Tapajós. As a final point, these techniques have a great potential and should be applied on the monitoring of protected areas.

Acknowledgements

The authors would like to thank INPE for giving the opportunity to improve skills in remote sensing, to CAPES and CNPq, for granting research scholarship; to Gabriela Banon and Camilo Rennó, Fabio Furlan Gama and Lênio Soares Galvão for the help.

References

- Adams, J. B.; Sabol, D.; Kapos, V.; Almeida Filho, R.; Roberts, D. A.; Smith, M. O.; & Gillespie, A. R (1995). Classification of multispectral images based on fractions of endmembers: Application to landcover change in the Brazilian Amazon. **Remote Sensing of Environment**, v.52, p. 137-154.
- Becker, B. K. **Amazônia: geopolítica na virada do III milênio**. Rio de Janeiro: Garamond, 2009.
- Figueira, A. M. S.; Miller, S. D.; Sousa, C. A. D.; Menton, M. C.; Maia, A. R.; da Rocha, H. R. ;Goulden, M. L. (2008). Effects of selective logging on tropical forest tree growth. **J. Geophys. Res.**, v.113, G00B05.
- IBAMA - Instituto brasileiro do meio ambiente e dos recursos naturais renováveis (2004). **Floresta Nacional do Tapajós - Plano de Manejo: Volume 1 - Informações Gerais**. 165 p. Disponível em:http://www.icmbio.gov.br/portal/images/stories/imgs-unidades-coservacao/flona_tapajoss.pdf. Acesso em: 04 ago. 2016.
- Kennedy, R. E.; Townsend, P. A.; Gross, J. E.; Cohen, W. B.; Bolstad, P.; Wang, Y.Q.; Adams, P. (2009). Remote sensing change detection tools for natural resource managers: Understanding concepts and tradeoffs in the design of landscape monitoring projects. **Remote Sensing of Environment**, v.113, p.1382–1396.
- Lu, D.; Li, G.; Moran, E.; Hetrick, S. (2014). Vegetation Change Detection in the Brazilian Amazon with Multitemporal Landsat Images. In: Wang, G.; Weng Q. (Org). **Remote Sensing of Natural Resources**. Oxford, UK: CRC Press, cap.7, p127-139.
- Potter, C. C.; Randerson, J. T.; Field, C. B.; Matson, P. A.; Vitousek, P. M.; Monney, H. A.; & Klooster, S. A (1993). Terrestrial ecosystem production: A process model based on global satellite and surface data. **Global Biogeochemical Cycles**, p. 811-841.
- Running, S. W.; Baldocchi, D. D.; Turner, D. P.; Gower, S. T.; Bakwin, P. S.; & Hibbard, K. A. (1999). A global terrestrial monitoring network integrating tower fluxes, flask sampling, ecosystem modeling and EOS satellite data. **Remote Sensing of Environment**, p. 108-127.
- Shimabukuro, Y.E.; Smith J.A. (1991). The least-squares mixing models to generate fractions images derived from remote sensing multispectral data. **IEEE Transactions on Geoscience and Remote Sensing**. v.29, n.1, p.16-20.
- Smith, M.O.; Adams, J.B.; Gillespie, A.R. (1990). Reference endmembers for spectral mixture analysis. **Australian Remote Sensing Conference**, v.1, p.331-340.